HHS Public Access

Author manuscript

FASEB J. Author manuscript; available in PMC 2023 April 13.

Published in final edited form as:

FASEB J. 2023 April ; 37(4): e22801. doi:10.1096/fj.202201368RR.

Charged multivesicular-body protein 4b forms complexes with gap-junction proteins during lens fiber cell differentiation

Yuefang Zhou[1], **Thomas M. Bennett**[1], **Thomas W. White**[2], **Alan Shiels**[1]

[1]Department of Ophthalmology and Visual Sciences, Washington University School of Medicine, St. Louis, MO, USA

[2]Department of Physiology and Biophysics, Stony Brook University, Stony Brook, NY, USA

Abstract

Charged multivesicular-body protein 4b (CHMP4B) is a core sub-unit of the endosomal sorting complex required for transport-III (ESCRT-III) machinery that serves myriad remodeling and scission processes of biological membranes. Mutation of the human CHMP4B gene underlies rare forms of early-onset lens opacities, or cataracts, and CHMP4B is required for lens growth and differentiation in mice. Here, we determine the sub-cellular distribution of CHMP4B in the lens and uncover a novel association with gap-junction alpha-3 protein (GJA3) or connexin-46 (Cx46) and GJA8 or Cx50. Immunofluorescence confocal microscopy revealed that CHMP4B localized to cell membranes of elongated fiber cells in the outer cortex of the lens - where large gap-junction plaques begin to form - particularly on the broad faces of these flattened hexagon-like cells in cross-section. Dual immunofluorescence imaging showed that CHMP4B co-localized with gap-junction plaques containing Cx46 and/or Cx50. When combined with the *in situ* proximity ligation assay, immunofluorescence confocal imaging indicated that CHMP4B lay in close physical proximity to Cx46 and Cx50. In Cx46-knockout (Cx46-KO) lenses, CHMP4B-membrane distribution was similar to that of wild-type, whereas, in Cx50-KO lenses CHMP4B localization to fiber cell membranes was lost. Immunoprecipitation and immunoblotting analyses revealed that CHMP4B formed complexes with Cx46 and Cx50 *in vitro*. Collectively, our data suggest that CHMP4B forms plasma-membrane complexes, either directly and/or indirectly, with gap-junction proteins Cx46 and Cx50 that are often associated with ‘ball-and-socket’ double-membrane junctions during lens fiber cell differentiation.

Keywords

Lens; fiber cell; gap-junction; ball-and-socket junction; connexin-46; connexin-50

Corresponding author: Alan Shiels, PhD, Ophthalmology and Visual Sciences, Box 8096, Washington University School of Medicine, 660 S. Euclid Ave., St. Louis, MO 63110, USA, Tel: 314-362-1637, shiels@wustl.edu.

AUTHOR CONTRIBUTIONS

Y. Zhou and A. Shiels conceived and designed the research; Y. Zhou and T.M. Bennett performed the research and acquired the data; T.W. White provided knock-out mice; Y. Zhou, T.M. Bennett, T.W. White, and A. Shiels analyzed and interpreted the data. A. Shiels wrote the first draft of the manuscript and all authors were involved in revising the final manuscript.

CONFLICT OF INTEREST STSTEMENT

The authors declare no conflicts of interest.

1. INTRODUCTION

The vertebrate lens is a transparent, highly-refractive cellular structure that plays a critical role in anterior eye development and fine-focusing of images onto the photosensitive retina.[1,2] At the cellular level, the lens is surrounded by a basement membrane or capsule containing an anterior monolayer of epithelial cells that divide and terminally differentiate throughout life into highly-elongated secondary fiber cells precisely organized into tightly packed, concentric layers or growth shells to form the refractive mass (nucleus and cortex) of the lens.[3,4] Lens fiber cells (LFCs) display a flattened-hexagonal cross-section with two broad cell-membrane surfaces that abut LFCs in adjacent growth-shells and four narrow faces that border LFCs in adjacent radial cell columns.[3,4] LFC differentiation is characterized by several coordinated processes - including cytoplasmic accumulation of crystallin proteins, plasma-membrane and actin-cytoskeleton remodeling, programmed organelle degradation, and core syncytium formation[3,5-8] that serve to establish and maintain a high refractive index and exquisite optical quality. Loss of lens transparency, or cataract(s), is often acquired with aging and, despite advances in surgical treatment, age-related cataract constitutes a leading cause of visual impairment (low vision and blindness) and a significant public healthcare burden worldwide.[9]

Prominent during LFC membrane remodeling is the accumulation of intercellular gap-junction channels, composed of gap-junction α3 protein (GJA3) or connexin 46 (Cx46) and GJA8 or Cx50, which share 88% amino-acid similarity and a similar 3D protein structure.[10-13] Gap-junction assembly involves oligomerization of six transmembrane connexin isoforms into homomeric (e.g., Cx46 or Cx50 isoforms) or heteromeric (e.g., Cx46 and Cx50 isoforms) hemi-channels, or connexons (i.e., hexamers), that dock in the extracellular space with connexons in neighboring cells to form homotypic (e.g., Cx46 or Cx50 connexons) or heterotypic (e.g., Cx46 and/or Cx50 connexons) intercellular channels with diverse gating properties that facilitate the cytoplasmic exchange of ions, small molecules, and fluids.[10] Cryo-electron microscopy, mass spectroscopy, and molecular dynamics simulation studies of native Cx46 and Cx50, purified from sheep lenses, have demonstrated that they co-assemble into a mixture of heteromeric and/or heterotypic intercellular channels in an open-pore conformation that is stabilized, in part, by membrane-lipid interactions.[13,14] LFC gap-junctions are arranged in large (micron-sized) two-dimensional arrays or plaques particularly on the broad cross-sectional membrane faces and are often associated with so called ‘ball-and-socket’ (B&S) double-membrane junctions that interlock cortical LFCs.[3,15-18] Loss-of-function studies in mice have shown that Cx46 and/or Cx50 are critical for lens growth, differentiation, and homeostasis, in part, by facilitating cell-cell adhesion and by providing an outflow pathway for the lens ion/fluid microcirculation system that is essential for maintaining the transparency and high refractive index of the avascular lens.[4,10,19,20] Sequence variations in the genes coding for Cx46 and Cx50 have been associated with both rare forms of inherited cataracts and frequently acquired forms of age-related cataracts in humans[12] (https://cat-map.wustl.edu) and gene-targeted mice that are homozygous for human Cx46 or Cx50 mutations develop cataracts associated with calcium bio-mineralization of the lens.[21-23]

Charged multivesicular-body proteins (CHMPs) comprise a phylogenetically conserved (Archaea-to-human) family of helical proteins (12 in humans, 11 in mice) that serve as core subunits of the endosomal sorting complex required for transport-III (ESCRT-III) machinery, which facilitates myriad biological membrane remodeling and scission processes.[24-28] These include, but are not limited to, multivesicular-body/-endosome (MVB/E) biogenesis[29,30], viral budding[31], cytokinetic (bridge) abscission[32], nuclear membrane sealing[33,34], plasma-membrane and lysosome-membrane repair[35-37], neuron pruning[38], autophagy[39], mitophagy[40], and ciliogenesis[41]. Structural studies have revealed that CHMP4B, or its conserved orthologs Snf7 (yeast) and Vps32 (*C. elegans*), can polymerize on cellular membranes with other ESCRT-III subunits to form spiral filaments that are recruited to the narrow necks of membrane bud-like structures in order to sever the vesicle-bud and reseal the parent membrane.[24-28] Like Cx46 and Cx50, sequence variations in the human gene for CHMP4B (*CHMP4B*) have been associated with inherited and age-related forms of cataracts in humans[42-46] (https://cat-map.wustl.edu). Heterologous overexpression studies suggest that a mutant form of CHMP4B (p.D129V), underlying early-onset cataract, impairs viral budding and inhibits chromatin binding in transformed cell-lines.[42,47] In mice, germline knockout or homozygous mutation of CHMP4B is embryonic lethal and conditional knock-down of CHMP4B in the lens resulted in severe inhibition of lens growth and fiber cell differentiation[48,49] - consistent with the importance of the ESCRT-III machinery in membrane dynamics including cytokinesis.[50] Beyond its association with human cataracts, little is known about CHMP4B function(s) in the lens. Here we provide the first evidence, to our knowledge, that CHMP4B forms complexes with gap-junction proteins Cx46 and Cx50 suggesting a novel role in lens cell-membrane differentiation.

2. MATERIALS AND METHODS

2.1. Mice

C57BL6/J (B6J) mice (Stock no. 000664), were obtained from The Jackson Laboratory (Bar Harbor, ME, USA). *Chmp4b*-floxed (*Chmp4b*$^{fx/fx}$) mice were generated by homologous recombination (B6J background) and bred with mice transgenic for lens-specific *Cre* recombinase (MLR10-*Cre*, generous gift from Dr. M.L. Robinson, Ohio State University)[51] to produce a conditional knock-down of *Chmp4b* in the lens (*Chmp4b*-CKD) along with control (*Chmp4b*$^{+/fx}$; *Cre*) mice as described.[49] Mice were genotyped for *Chmp4b*-allele and *Cre*-transgene status by polymerase chain reaction (PCR) amplification of toe or ear biopsy genomic DNA using gene-specific primers (Supplemental Table 1) as described.[49,52] Cx46/*Gja3* knock-out (KO) and Cx50/*Gja8*-KO mice were generated by homologous recombination and Cx46 and Cx50 allele status were confirmed by PCR-genotyping as described.[53-55] All experimental mouse strains were maintained on the B6J genetic background to avoid a deletion mutation in the gene for lens beaded filament structural protein-2 (*Bfsp2*) carried by certain inbred strains.[56,57] Mice were humanely euthanized according to the American Veterinary Medical Association (AVMA) guidelines and the eyes removed. All mouse studies were approved by the Institutional Animal Care and Use Committee (IACUC) at Washington University in compliance with the Institute for Laboratory Animal Research (ILAR) guidelines.

2.2. CHMP4B antibody production and validation

A custom-synthesized, synthetic-peptide from the carboxy-terminus of CHMP4B was used to generate an affinity-purified polyclonal antibody (#PA0518) using standard immunological techniques in rabbits (Open Biosystems, Huntsville, AL). Antibody specificity was validated by using small interfering RNA (siRNA)-mediated knockdown of CHMP4B (Accell Human CHMP4B siRNA - SMARTpool, Dharmacon, Lafayette, CO) in cultured (37°C, 5% CO_2) HEK-293T cells (CRL-3216, ATCC, Manassas, VA) according to the manufacturers' instructions. Briefly, HEK293 cells (~50% confluent in 24-well plates) were transfected (72 hours) with CHMP4B siRNA or negative-control ('scrambled') siRNA (Accell Green Non-targeting, Dharmacon), each at 1 μM in 500 ul Accell Delivery Media, then refed with fresh culture media (Minimal Essential Media/MEM, 20% Fetal Bovine Serum/FBS Gibco, ThermoFisher Scientific, Waltham, MA, USA). Silenced cells were harvested (rinsed in PBS, detached in 0.02% EDTA, centrifuged 1500 x g, 5 min) 24 hrs later and cell pellets lysed by resuspension in 1% IGEPAL (C-630, Sigma-Aldrich, St. Louis, MO, USA). Lysate protein concentration was measured using the Non-interfering assay (G-Bioscience, St. Louis, MO) and 5 μg of soluble protein used for immunoblotting as described.[58,59]

2.3. Immunofluorescence confocal microscopy (IFCM)

Enucleated eyes were fixed (6 hours, 4°C) in 4% paraformaldehyde (PFA, #15710, Electron Microscopy Sciences, EMS, Hatfield, PA) diluted in phosphate buffered saline (PBS, #P4417-100TAB, Sigma-Aldrich) and processed using standard formaldehyde-fixed-paraffin-embedded (FFPE) serial-section techniques. Single LFCs were gently dissected from the outer cortical region of fixed (4% PFA, 5 hours) lenses bisected along the optical axis, then dried on to polylysine-coated slides, permeabilized, and blocked as described.[60] IFCM was performed using commercially-available primary antibodies (Supplemental Table 2) and species-appropriate Alexa-fluor conjugated secondary antibodies (ThermoFisher Scientific), counterstaining of cell-nuclei with 4′,6-diamidino-2-phenylindole (DAPI; MilliporeSigma, Burlington, MA, USA) and cell-membranes with rhodamine-based wheat-germ agglutinin (WGA) conjugates (RL-1022, Vector Laboratories, Newark, CA, USA; CF 640R, Biotium, Freemont, CA, USA), followed by confocal scanning microscopy (FV1000, Olympus, Center Valley, PA, USA; Zeiss LSM 800 with Airyscan, Carl Zeiss, White Plains, NY, USA) as described.[49,52,58,61] For fluorescence image co-localization analysis, dual-immunofluorescence signals from at least 3 images from 6 lens sections of 3 mice (≥ 18 images/genotype) or from 1 image from 12 single LFCs of 3 mice were analyzed using the Fiji distribution of open source ImageJ software and quantified using the Just Another Co-localization Plugin (JACoP) of the Bioimaging and Optics Platform (BIOP) with Otsu's auto-threshold selection method to calculate Pearson's correlation coefficient as described.[62-64]

2.4. *In situ* proximity ligation assay (PLA)

PLA was performed using the Duolink *In Situ* Detection Reagents Orange kit (DUO92106 Sigma-Aldrich) according to the manufacturers' instructions and as described.[65] Briefly, pre-blocked sections were incubated (16 hr, 4°C) with primary antibodies (Supplemental

Table 2) raised in different species (rabbit anti-CHMP4B and goat anti-Cx46 or goat anti-Cx50), washed (2 x 5 min), re-incubated (1 hr, 37°C) with anti-goat Plus and anti-rabbit Minus PLA probes, followed by ligation (30 min, 37°C), and amplification (100 min, 37°C) prior to fluorescence confocal microscopy (FV1000). For quantification, PLA positive signals from at least one image from 6 lens sections of 3 mice (≥ 6 images/genotype) were analyzed for particle number (average counts) using Fiji software.[63,64] Non-specific background threshold and true particle size threshold were selected using control lens sections from Cx46-KO and Cx50-KO mice and from wild-type mice using only one of the paired PLA antibodies.

2.5. Immunoprecipitation and immunoblotting

Immunoprecipitation was performed using the Pierce Classic IP Kit (#26146, ThermoFisher Scientific) with appropriate primary antibodies (Supplemental Table 2) according to the manufacturer's instructions and as described.[58] Immunoblot analysis was performed with appropriate primary antibodies (Supplemental Table 2) and IRDye labelled secondary antibodies using the Odyssey Infrared Imaging System (Li-Cor, Lincoln, NE, USA) according to the manufacturer's instructions and as described[58,59]

2.6. Statistical analysis

One-way analysis of variance (ANOVA) was used to determine statistical significance (P) ± standard error (SE) of Pierson's correlation coefficient.

3. RESULTS

3.1. CHMP4B localizes to LFC-membranes

To determine the distribution of CHMP4B in the lens, we undertook immunofluorescence confocal microscopy (IFCM) using a synthetic-peptide antibody that was validated for CHMP4B specificity by siRNA-mediated knockdown and immunoblotting techniques (Supplemental Figure 1). Using this primary antibody for IFCM, we have localized CHMP4B specifically to the outer cortex (~ 50-100 μm depth from equatorial surface) of the wild-type mouse lens with intense, punctate, labeling mostly on the broad cross-sectional faces of secondary LFC membranes (Figure 1). By contrast, we have not observed CHMP4B localization to cell-membranes of lens epithelial cells that often line the peripheral edges of lens sections suggesting that CHMP4B localization to cell-membranes was associated with differentiation of LFCs from lens epithelial cells.

In order to further validate localization of CHMP4B to LFC membranes we sought to generate *Chmp4b*-deficient lenses by crossing *Chmp4b*-floxed mice[49] with transgenic, lens-specific MLR10-*Cre* mice that express *Cre*-recombinase under the control of a modified αA-crystallin gene promoter.[51] During lens development, MLR10-*Cre* expression commences in the lens vesicle and primary fiber cells at embryonic day 10.5 (E10.5) progressing to all lens epithelial cells and secondary fiber cells by E12.5. IFCM imaging confirmed localization of CHMP4B to LFC membranes in control (*Chmp4b*$^{+/fx}$; *Cre*) lenses at postnatal-day 1 (P1) (Supplemental Figure 2A). By contrast, there was a significant loss of CHMP4B-membrane localization in *Chmp4b*-deficient lenses particularly within the

lens core or nucleus at P1 (Supplemental Figure 2B-D). However, some CHMP4B-positive membrane-labeling was observed toward the peripheral cortex of *Chmp4b*-deficient lenses at P1 (Supplemental Figure 2B-D). In previous studies, we have shown that *Chmp4b*-deficient lenses display highly variable degrees of lens dysmorphology, including lens ablation, suggesting that MLR10-*Cre* deletion of *Chmp4b* was non-uniform or mosaic across the lens (at least on the B6J background) - consistent with a conditional knockdown.[49] We note that MLR10 transgenic mice lack *Cre*-recombinase protein in the lens epithelium at E15.5 and may exhibit incomplete recombination with some floxed alleles in the lens epithelium[66] - raising the possibility that *Chmp4b* expression may recover, after conditional knockdown, to rescue nascent LFC differentiation. Regardless, these data suggest that CHMP4B function is required for lens growth and differentiation, in part, through localization to LFC-membranes.

3.2. CHMP4B co-localizes with gap-junction proteins Cx46 and Cx50 in the lens

Gap-junctions composed of Cx46 and/or Cx50 are known to form large plaques particularly on the broad cross-sectional surfaces of LFC-membranes.[3,15,16] In addition, both Cx46 and Cx50 gap-junction plaques have been localized to B&S double-membrane junctions that interlock cortical LFCs.[15,17,18] Since CHMP4B localization resembled that of gap-junction plaques on LFC membranes, we performed dual-antibody IFCM to compare the distribution of CHMP4B with that of Cx46 and Cx50. Dual-antibody imaging suggested that CHMP4B predominantly co-localized with Cx46 and Cx50 containing gap-junction plaques particularly on the broad cross-sectional faces of LFC membranes where B&S junctions are also found (Figure 2). Quantification of the dual-immunofluorescence signals using Pearson's correlation coefficient (PCC) indicated that CHMP4B was approximately 70% co-localized with Cx46 and Cx50 in wild-type lenses [Figure 2G]. In order to visualize CHMP4B and gap-junction plaques 'face-on' in the superficial plane, rather than in cross-section, we performed dual-antibody IFCM imaging of single LFCs isolated from the peripheral cortex of wild-type lenses. Supplemental Figure 3 shows predominant co-localization of CHMP4B with large plaques of Cx46 (PCC = 0.57 ± SE 0.028) mostly on the broad faces of single LFC membranes. Mechanical disruption of gap-junction plaques during isolation of single LFCs may have contributed to the reduced co-localization of CHMP4B and Cx46 compared to that observed in whole lens sections. Nevertheless, our data provide the first evidence, to our knowledge, that CHMP4B co-localizes with Cx46 and Cx50 containing gap-junction plaques and B&S junctions found on LFC membranes.

3.3. CHMP4B forms complexes with gap-junction proteins Cx46 and Cx50 in the lens and in vitro

Since the lens phenotypes of Cx46-KO and Cx50-KO mice[67] are less severe than that of *Chmp4b*-deficient mice (Supplemental Figure 2)[49], we sought to model the effects of Cx46 and/or Cx50 loss-of-function on CHMP4B localization in the lens. In Cx46-KO lenses, CHMP4B was mostly localized to punctate 'ladder-like' regions on the broad faces of LFC membranes similar to that of Cx46 in wild-type lenses (Figure 3A-F) and to Cx50 in both wild-type and Cx46-KO lenses (Figure 4A-F). By contrast, in Cx50-KO lenses CHMP4B exhibited diffuse cytoplasmic labeling (Figure 3G, I, Figure 4G, I), whereas, Cx46 displayed a more uniform membrane distribution in Cx50-KO lenses (Figure 3H, I) compared to

the punctate pattern in wild-type (Figure 3 B, C) - consistent with a previous report.[17] In Cx46 and Cx50 double knock-out (Cx46/50-DKO) lenses, the diffuse CHMP4B labeling of the cytoplasm resembled that found in Cx50-KO lenses (Figure 3G, I, J, L, Figure 4G, I, J, L). Quantification of the dual-immunofluorescence signals using PCC confirmed that CHMP4B was ~ 70% co-localized with Cx50 in Cx46-KO lenses, similar to that in wild-type lenses, whereas, CHMP4B exhibited minimal co-localization with Cx46 in Cx50-KO and Cx46/50-DKO lenses [Figure 3M and Fig. 4M]. Overall, these observations suggest that in the absence of Cx50 CHMP4B had redistributed from its active (open) state - as a polymer on the membrane - to its auto-inhibited (closed) state - as a soluble monomer in the cytoplasm.[68]

In order to estimate the physical distance between CHMP4B and gap-junction proteins on LFC-membranes, we performed the *in situ* PLA with primary antibodies raised in different species. Subsequent IFCM imaging revealed that both CHMP4B-Cx46 and CHMP4B-Cx50 complexes were present on wild-type LFC-membranes (Figure 5A, B). By contrast, CHMP4B-Cx46 membrane complexes were absent from Cx46-KO and Cx50-KO lenses (Figure 5C, E), whereas, CHMP4B-Cx50 membrane complexes were present in Cx46-KO lenses and absent from Cx50-KO lenses (Figure 5D, F). Quantification of PLA images confirmed that the number of positive signals for CHMP4B-Cx46 membrane complexes was significantly greater in wild-type lenses compared to Cx46-KO or Cx50-KO lenses, whereas, signals for CHMP4B-Cx50 membrane complexes were significantly greater in wild-type and Cx46-KO lenses compared to Cx50-KO lenses [Figure 5G]. PLA is a more stringent test of co-localization than conventional dual-antibody labeling and is more sensitive to differences in the antigen affinity and/or avidity of the Cx46 and Cx50 antibodies used. Such differences likely contributed to a reduced PLA co-localization signal compared with that of dual-antibody co-localization (compare Figures 2 and 5) and may also account for the reduced CHMP4B-Cx50 PLA signals in wild-type lenses compared to those of CHMP4B-Cx46 [Figure 5G]. Regardless, our PLA data suggest that at least a sub-population of CHMP4B lay in close proximity (< 40-nm apart) to Cx46 and/or Cx50 and further supported the requirement of Cx50, but not Cx46, for CHMP4B localization to LFC-membranes.

To demonstrate that CHMP4B formed complexes with Cx46 and Cx50 *in vitro*, we performed immunoprecipitation and immunoblotting analyses. CHMP4B complexes with Cx46 and Cx50 were present in wild-type lens lysates (Figure 6). By contrast, while Cx46-KO lens lysates contained CHMP4B-Cx50 complexes, CHMP4B-Cx46 complexes were absent from Cx50-KO lens extracts (Figure 6). In addition, CHMP4B complexes with several other LFC-membrane proteins including, lens major intrinsic protein or aquaporin-0 (MIP/AQP0), catenin beta-1 (CTNNB1), and N-cadherin or cadherin-2 (CDH2) were absent in wild-type lens extracts (Supplemental Figure 4). Overall, our combined *in situ* immuno-imaging and *in vitro* immuno-precipitation data suggest that CHMP4B specifically forms complexes with Cx46 and Cx50 and that Cx46 is not required for CHMP4B-Cx50 complex formation, whereas, Cx50 is required for CHMP4B-Cx46 complex formation on LFC membranes.

4. DISCUSSION

CHMP4B serves as a core subunit of the ESCRT-III bio-membrane remodeling and scission machinery and has been associated with inherited and age-related cataracts in humans and lens growth deficiency and dysmorphology in mice.[42-46,49] In this study we discovered that CHMP4B forms complexes with gap-junction proteins Cx46 and Cx50 on LFC-membranes (Figures 1-5) and *in vitro* (Figure 6). Further, loss of Cx50 - but not Cx46 - in the lens resulted in redistribution of CHMP4B from LFC-membranes to the cytoplasm (Figures 3-5) and loss of CHMP4B-Cx50 complexes *in vitro* (Figure 6). At least a sub-population of CHMP4B on LFC membranes was found to lie in close proximity to Cx46 and/or Cx50 (Figure 5) - suggesting possible protein-protein interactions. Although Cx50 has been reported to interact with MIP/AQP0,[20] we did not find CHMP4B-MIP/AQP0 complexes in wild-type lenses (Supplemental Figure 4). Whether or not CHMP4B interacts with Cx46 and Cx50 either directly and/or indirectly via an intermediate protein(s) remains to be determined. Overall, our data suggest that Cx50, but not Cx46, is required for CHMP4B complex formation on LFC membranes. Such complex-formation between CHMP4B, Cx46, and Cx50 in the outer cortex of the mouse lens provides a spatiotemporal overlap with (1) the sub-capsular and cortical lens opacities observed in human *CHMP4B*-related cataract[42,43,69,70] and (2) the formation of large gap-junction plaques that are often associated with B&S double-membrane interlocking junctions on the broad cross-sectional surfaces of LFC-membranes.[15-18]

Although complex formation between the ESCRT-III protein CHMP4B and connexins on LFC membranes was unexpected, previous studies have identified two other ESCRT proteins that are associated with connexin degradation. The ubiquitin-binding protein tumor susceptibility gene 101 (TSG101) has been shown to interact with the C-termini of several connexins including Cx43.[71] Similarly, another ubiquitin-binding protein hepatocyte growth factor-regulated tyrosine kinase substrate (HRS), along with TSG101, have been shown to be important for trafficking of ubiquitinated Cx43 to lysosomes for degradation.[71-73] We note that Cx43 is expressed in lens epithelial cells that line the anterior surface of the lens but not in LFCs that form the refractive mass of the lens.[11,12] HRS and TSG101 are components of the ESCRT-0 and ESCRT-1 machinery, respectively, and sequential recruitment of ESCRT-0, ESCRT-I, and ESCRT-II, precedes that of the ESCRT-III machinery to the endosomal membranes before fusion with lysosomes.[30] CHMP4B is known to play canonical roles in both of the lysosomal degradation pathways that contribute to gap-junction/connexin degradation including Cx43 and Cx50.[73,74] In the endo-lysosomal pathway, CHMP4B/ESCRT-III participates in the formation of intraluminal vesicles found in MVB/Es that subsequently fuse with lysosomes.[30] Similarly, CHMP4B/ESCRT-III participates in several phago-lysosomal or autophagy pathways including the formation of MVB/Es that fuse with autophagosomes to form amphisomes prior to lysosome fusion in macroautophagy, endosomal and lysosomal microautophagy, and phagophore closure during mitophagy.[39,40] Further, CHMP4B deficiency in cortical neurons has been shown to result in accumulation of autophagosomes.[48] However, it remains to be determined whether or not recruitment of CHMP4B to Cx46 and Cx50 gap-junctions on LFC-membranes is solely for the purpose of lysosomal degradation.

It is well established that Cx46 and Cx50 serve critical yet non-redundant functions in the lens.[67] While lenses lacking either Cx46 or Cx50 developed nuclear cataracts of varying severity influenced by genetic background, only loss of Cx50 resulted in a significantly smaller lens (~ 46% loss of mass compared to wild-type) regardless of background.[53,54,75,76] Further, while replacement of Cx50 by knock-in of Cx46 (Cx50KICx46) mitigated cataract formation it failed to rescue lens growth deficiency and both Cx50-KO and Cx50KICx46 lenses have been shown to contain fewer cells due to reduced postnatal lens cell proliferation.[77,78] Our previous studies have shown that CHMP4B-deficiency in the lens resulted in severe inhibition of lens growth and LFC differentiation[49] and, here, we have shown that CHMP4B is lost from LFC membranes in the absence of Cx50 (Fig. 3-5). Thus, it is conceivable that loss of CHMP4B from LFC-membranes directly contributes to growth inhibition of Cx50-KO lenses. In addition to deficient lens growth, loss of Cx50 also resulted in small disorganized Cx46 gap-junction plaques, whereas, loss of Cx46 did not impair Cx50 gap-junction plaque formation.[17,18] Collectively, these observations suggest a synergistic role for CHMP4B and Cx50 in LFC gap-junction plaque formation and normal lens growth.

In addition to gap-junction plaque formation, Cx46 and Cx50 have been associated with B&S double-membrane, junctional domains that interlock adjacent LFCs and are believed to provide rapid cytoplasmic exchange of ions, small solutes, and fluids coupled with cell-cell adhesion and mechanical integrity during rapid LFC elongation.[15,17,18,20] B&S junctions are characterized by neck and head-like regions (0.5-2 μm diameter) of plasma-membrane curvature that protrude from one LFC into neck-and-head-like invaginations in opposing LFC membranes - in a manner similar to jig-saw pieces. In addition to Cx46 and Cx50, several other proteins have been associated with B&S structures including zonula occludens-1 (ZO-1), beta-dystroglycan (β-DG), and unidentified Postsynaptic density protein, Drosophila disc large tumor suppressor, Zonula occludens-1 protein (PDZ)-domain containing proteins.[17,18] Notably, Cx50 has been shown to require an intact PDZ-binding motif and ZO-1 in order to form functional gap-junction channels.[79] Lenses lacking Cx50 have been associated with loss of mature B&S junctions and disruption of F-actin distribution in differentiating LFCs, whereas, lenses lacking Cx46 retain mature B&S junctions and F-actin distribution.[17] However, lenses in which Cx46 replaced Cx50 exhibited only partial rescue of B&S-like structures suggesting that Cx50 was predominantly required for B&S junction formation.[18] Recently, CHMP4B has been shown to associate with F-actin during the assembly of primary cilia and is required for structural integrity of the ciliary membrane.[41] Since CHMP4B has been associated with numerous sub-cellular processes involving membrane curvature, including plasma-membrane budding and repair,[35] it is conceivable that CHMP4B-Cx50 containing complexes are required for the assembly of gap-junction rich B&S interlocking domains on LFC membranes.

In summary, our data reveal novel complex-formation between the ESCRT-III protein CHMP4B and gap-junction proteins Cx46 and Cx50 on LFC membranes and *in vitro*. Further studies will be required to characterize the roles of (1) the endo-lysosomal versus autophagy pathways in Cx46 and Cx50 turnover and/or degradation, (2) direct versus indirect CHMP4B interactions with Cx46, Cx50, and/or other membrane-associated proteins (e.g., ESCRT-III proteins) in gap-junction plaque formation, and (3) CHMP4B-

Cx50 containing complexes in B&S double-membrane junction formation during LFC differentiation.

Supplementary Material

Refer to Web version on PubMed Central for supplementary material.

ACKNOWLEDGEMENTS

We thank G. Ling for eye histology support and Dr. M.L. Robinson for sharing MLR10-*Cre* mice. This work was supported by NIH/NEI grants EY028899 and EY012284 (to AS), EY026911 (to TWW), EY02687 (Core Grant for Vision Research), and an unrestricted grant to the Department of Ophthalmology and Visual Sciences from Research to Prevent Blindness.

DATA AVAILIBILITY STATEMENT

The data that support the findings of this study are available in the methods and/or supplementary material of this article.

Abbreviations:

CHMP	charged multi-vesicular body protein
ESCRT	endosome sorting complex required for transport
MVB/E	multivesicular-body/endosome
LFC	lens fiber cell
B&S	ball-and-socket
IFCM	immunofluorescence confocal microscopy
PLA	proximity ligation assay
WGA	wheat-germ agglutinin
DAPI	4′,6-diamidino-2-phenylindole

References

1. Beebe DC, Coats JM. The lens organizes the anterior segment: specification of neural crest cell differentiation in the avian eye. Dev Biol 2000;220(2):424–31. doi: 10.1006/dbio.2000.9638 [PubMed: 10753528]
2. Iribarren R Crystalline lens and refractive development. Prog Retin Eye Res 2015;47:86–106. doi: 10.1016/j.preteyeres.2015.02.002 [PubMed: 25683786]
3. Bassnett S, Shi Y, Vrensen GF. Biological glass: structural determinants of eye lens transparency. Philos Trans R Soc Lond B Biol Sci 2011;366(1568):1250–64. doi: 10.1098/rstb.2010.0302 [PubMed: 21402584]
4. Donaldson PJ, Grey AC, Maceo Heilman B, et al. The physiological optics of the lens. Prog Retin Eye Res 2017;56:e1–e24. doi: 10.1016/j.preteyeres.2016.09.002 [PubMed: 27639549]
5. Cvekl A, Ashery-Padan R. The cellular and molecular mechanisms of vertebrate lens development. Development 2014;141(23):4432–47. doi: 10.1242/dev.107953 [PubMed: 25406393]

6. Cheng C, Nowak RB, Fowler VM. The lens actin filament cytoskeleton: Diverse structures for complex functions. Exp Eye Res 2017;156:58–71. doi: 10.1016/j.exer.2016.03.005 [PubMed: 26971460]
7. Cvekl A, Zhang X. Signaling and Gene Regulatory Networks in Mammalian Lens Development. Trends Genet 2017;33(10):677–702. doi: 10.1016/j.tig.2017.08.001 [PubMed: 28867048]
8. Morishita H, Eguchi T, Tsukamoto S, et al. Organelle degradation in the lens by PLAAT phospholipases. Nature 2021;592(7855):634–38. doi: 10.1038/s41586-021-03439-w [published Online First: 2021/04/16] [PubMed: 33854238]
9. GBD 2019, Blindness and Vision Impairment Collaborators, Vision Loss Expert Group of the Global Burden of Disease Study. Causes of blindness and vision impairment in 2020 and trends over 30 years, and prevalence of avoidable blindness in relation to VISION 2020: the Right to Sight: an analysis for the Global Burden of Disease Study. Lancet Glob Health 2021;9(2):e144–e60. doi: 10.1016/S2214-109X(20)30489-7 [published Online First: 2020/12/05] [PubMed: 33275949]
10. Mathias RT, White TW, Gong X. Lens gap junctions in growth, differentiation, and homeostasis. Physiol Rev 2010;90(1):179–206. doi: 10.1152/physrev.00034.2009 [published Online First: 2010/01/21] [PubMed: 20086076]
11. Berthoud VM, Minogue PJ, Osmolak P, et al. Roles and regulation of lens epithelial cell connexins. FEBS Lett 2014;588(8):1297–303. doi: 10.1016/j.febslet.2013.12.024 [published Online First: 2014/01/18] [PubMed: 24434541]
12. Berthoud VM, Ngezahayo A. Focus on lens connexins. BMC Cell Biol 2017;18(Suppl 1):6. doi: 10.1186/s12860-016-0116-6 [published Online First: 2017/01/27] [PubMed: 28124626]
13. Myers JB, Haddad BG, O'Neill SE, et al. Structure of native lens connexin 46/50 intercellular channels by cryo-EM. Nature 2018;564(7736):372–77. doi: 10.1038/s41586-018-0786-7 [published Online First: 2018/12/14] [PubMed: 30542154]
14. Flores JA, Haddad BG, Dolan KA, et al. Connexin-46/50 in a dynamic lipid environment resolved by CryoEM at 1.9 A. Nat Commun 2020;11(1):4331. doi: 10.1038/s41467-020-18120-5 [published Online First: 2020/08/30] [PubMed: 32859914]
15. Biswas SK, Lee JE, Brako L, et al. Gap junctions are selectively associated with interlocking ball-and-sockets but not protrusions in the lens. Mol Vis 2010;16:2328–41. [published Online First: 2010/12/09] [PubMed: 21139982]
16. Cheng C, Nowak RB, Gao J, et al. Lens ion homeostasis relies on the assembly and/or stability of large connexin 46 gap junction plaques on the broad sides of differentiating fiber cells. Am J Physiol Cell Physiol 2015;308(10):C835–47. doi: 10.1152/ajpcell.00372.2014 [published Online First: 2015/03/06] [PubMed: 25740157]
17. Wang E, Geng A, Maniar AM, et al. Connexin 50 Regulates Surface Ball-and-Socket Structures and Fiber Cell Organization. Invest Ophthalmol Vis Sci 2016;57(7):3039–46. doi: 10.1167/iovs.16-19521 [published Online First: 2016/06/10] [PubMed: 27281269]
18. Wang E, Geng A, Seo R, et al. Knock-in of Cx46 partially rescues fiber defects in lenses lacking Cx50. Mol Vis 2017;23:160–70. [published Online First: 2017/05/02] [PubMed: 28458505]
19. Gu S, Biswas S, Rodriguez L, et al. Connexin 50 and AQP0 are Essential in Maintaining Organization and Integrity of Lens Fibers. Invest Ophthalmol Vis Sci 2019;60(12):4021–32. doi: 10.1167/iovs.18-26270 [published Online First: 2019/09/29] [PubMed: 31560767]
20. Li Z, Quan Y, Gu S, et al. Beyond the Channels: Adhesion Functions of Aquaporin 0 and Connexin 50 in Lens Development. Front Cell Dev Biol 2022;10:866980. doi: 10.3389/fcell.2022.866980 [published Online First: 2022/04/26] [PubMed: 35465319]
21. Gao J, Minogue PJ, Beyer EC, et al. Disruption of the lens circulation causes calcium accumulation and precipitates in connexin mutant mice. Am J Physiol Cell Physiol 2018;314(4):C492–C503. doi: 10.1152/ajpcell.00277.2017 [published Online First: 2018/01/20] [PubMed: 29351411]
22. Berthoud VM, Gao J, Minogue PJ, et al. The Connexin50D47A Mutant Causes Cataracts by Calcium Precipitation. Invest Ophthalmol Vis Sci 2019;60(6):2336–46. doi: 10.1167/iovs.18-26459 [published Online First: 2019/05/23] [PubMed: 31117126]

23. Berthoud VM, Gao J, Minogue PJ, et al. Connexin Mutants Compromise the Lens Circulation and Cause Cataracts through Biomineralization. Int J Mol Sci 2020;21(16) doi: 10.3390/ijms21165822 [published Online First: 2020/08/23]
24. Hurley JH. ESCRTs are everywhere. EMBO J 2015;34(19):2398–407. doi: 10.15252/embj.201592484 [published Online First: 2015/08/28] [PubMed: 26311197]
25. McCullough J, Frost A, Sundquist WI. Structures, Functions, and Dynamics of ESCRT-III/Vps4 Membrane Remodeling and Fission Complexes. Annu Rev Cell Dev Biol 2018;34:85–109. doi: 10.1146/annurev-cellbio-100616-060600 [published Online First: 2018/08/11] [PubMed: 30095293]
26. Vietri M, Radulovic M, Stenmark H. The many functions of ESCRTs. Nat Rev Mol Cell Biol 2020;21(1):25–42. doi: 10.1038/s41580-019-0177-4 [published Online First: 2019/11/11] [PubMed: 31705132]
27. Remec Pavlin M, Hurley JH. The ESCRTs - converging on mechanism. J Cell Sci 2020;133(18) doi: 10.1242/jcs.240333 [published Online First: 2020/09/18]
28. Olmos Y The ESCRT Machinery: Remodeling, Repairing, and Sealing Membranes. Membranes (Basel) 2022;12(6) doi: 10.3390/membranes12060633 [published Online First: 2022/06/24]
29. Babst M, Katzmann DJ, Estepa-Sabal EJ, et al. Escrt-III: an endosome-associated heterooligomeric protein complex required for mvb sorting. Dev Cell 2002;3(2):271–82. [PubMed: 12194857]
30. Hanson PI, Cashikar A. Multivesicular body morphogenesis. Annu Rev Cell Dev Biol 2012;28:337–62. doi: 10.1146/annurev-cellbio-092910-154152 [PubMed: 22831642]
31. Scourfield EJ, Martin-Serrano J. Growing functions of the ESCRT machinery in cell biology and viral replication. Biochem Soc Trans 2017;45(3):613–34. doi: 10.1042/BST20160479 [PubMed: 28620025]
32. Stoten CL, Carlton JG. ESCRT-dependent control of membrane remodelling during cell division. Semin Cell Dev Biol 2018;74:50–65. doi: 10.1016/j.semcdb.2017.08.035 [PubMed: 28843980]
33. Vietri M, Schink KO, Campsteijn C, et al. Spastin and ESCRT-III coordinate mitotic spindle disassembly and nuclear envelope sealing. Nature 2015;522(7555):231–5. doi: 10.1038/nature14408 [PubMed: 26040712]
34. Olmos Y, Hodgson L, Mantell J, et al. ESCRT-III controls nuclear envelope reformation. Nature 2015;522(7555):236–9. doi: 10.1038/nature14503 [PubMed: 26040713]
35. Jimenez AJ, Maiuri P, Lafaurie-Janvore J, et al. ESCRT machinery is required for plasma membrane repair. Science 2014;343(6174):1247136. doi: 10.1126/science.1247136 [PubMed: 24482116]
36. Skowyra ML, Schlesinger PH, Naismith TV, et al. Triggered recruitment of ESCRT machinery promotes endolysosomal repair. Science 2018;360(6384) doi: 10.1126/science.aar5078 [published Online First: 2018/04/07]
37. Radulovic M, Schink KO, Wenzel EM, et al. ESCRT-mediated lysosome repair precedes lysophagy and promotes cell survival. EMBO J 2018;37(21) doi: 10.15252/embj.201899753
38. Loncle N, Agromayor M, Martin-Serrano J, et al. An ESCRT module is required for neuron pruning. Sci Rep 2015;5:8461. doi: 10.1038/srep08461 [PubMed: 25676218]
39. Lefebvre C, Legouis R, Culetto E. ESCRT and autophagies: Endosomal functions and beyond. Semin Cell Dev Biol 2018;74:21–28. doi: 10.1016/j.semcdb.2017.08.014 [PubMed: 28807884]
40. Zhen Y, Spangenberg H, Munson MJ, et al. ESCRT-mediated phagophore sealing during mitophagy. Autophagy 2019:1–16. doi: 10.1080/15548627.2019.1639301 [published Online First: 2019/08/02]
41. Jung E, Choi TI, Lee JE, et al. ESCRT subunit CHMP4B localizes to primary cilia and is required for the structural integrity of the ciliary membrane. FASEB J 2020;34(1):1331–44. doi: 10.1096/fj.201901778R [published Online First: 2020/01/10] [PubMed: 31914703]
42. Shiels A, Bennett TM, Knopf HL, et al. CHMP4B, a novel gene for autosomal dominant cataracts linked to chromosome 20q. Am J Hum Genet 2007;81(3):596–606. doi: 10.1086/519980 [PubMed: 17701905]
43. Zhang XH, Da Wang J, Jia HY, et al. Mutation profiles of congenital cataract genes in 21 northern Chinese families. Mol Vis 2018;24:471–77. [PubMed: 30078984]

44. Jackson D, Malka S, Harding P, et al. Molecular diagnostic challenges for non-retinal developmental eye disorders in the United Kingdom. Am J Med Genet C Semin Med Genet 2020;184(3):578–89. doi: 10.1002/ajmg.c.31837 [published Online First: 2020/08/25] [PubMed: 32830442]
45. Wang X, Wang D, Wang Q, et al. Broadening the Mutation Spectrum in GJA8 and CHMP4B: Novel Missense Variants and the Associated Phenotypes in Six Chinese Han Congenital Cataracts Families. Front Med (Lausanne) 2021;8:713284. doi: 10.3389/fmed.2021.713284 [published Online First: 2021/11/02] [PubMed: 34722561]
46. Yonova-Doing E, Zhao W, Igo RP Jr., et al. Common variants in SOX-2 and congenital cataract genes contribute to age-related nuclear cataract. Commun Biol 2020;3(1):755. doi: 10.1038/s42003-020-01421-2 [published Online First: 2020/12/15] [PubMed: 33311586]
47. Sagona AP, Nezis IP, Stenmark H. Association of CHMP4B and autophagy with micronuclei: implications for cataract formation. Biomed Res Int 2014;2014:974393. doi: 10.1155/2014/974393 [PubMed: 24741567]
48. Lee JA, Beigneux A, Ahmad ST, et al. ESCRT-III dysfunction causes autophagosome accumulation and neurodegeneration. Curr Biol 2007;17(18):1561–7. doi: 10.1016/j.cub.2007.07.029 [PubMed: 17683935]
49. Zhou Y, Bennett TM, Shiels A. A charged multivesicular body protein (CHMP4B) is required for lens growth and differentiation. Differentiation 2019;109:16–27. doi: 10.1016/j.diff.2019.07.003 [published Online First: 2019/08/14] [PubMed: 31404815]
50. Gulluni F, Prever L, Li H, et al. PI(3,4)P2-mediated cytokinetic abscission prevents early senescence and cataract formation. Science 2021;374(6573):eabk0410. doi: 10.1126/science.abk0410 [published Online First: 2021/12/10] [PubMed: 34882480]
51. Zhao H, Yang Y, Rizo CM, et al. Insertion of a Pax6 consensus binding site into the alphaA-crystallin promoter acts as a lens epithelial cell enhancer in transgenic mice. Invest Ophthalmol Vis Sci 2004;45(6):1930–9. [PubMed: 15161860]
52. Zhou Y, Bennett TM, Shiels A. Lens ER-stress response during cataract development in Mip-mutant mice. Biochim Biophys Acta 2016;1862(8):1433–42. doi: 10.1016/j.bbadis.2016.05.003 [PubMed: 27155571]
53. Gong X, Li E, Klier G, et al. Disruption of alpha3 connexin gene leads to proteolysis and cataractogenesis in mice. Cell 1997;91(6):833–43. doi: 10.1016/s0092-8674(00)80471-7 [published Online First: 1997/12/31] [PubMed: 9413992]
54. White TW, Goodenough DA, Paul DL. Targeted ablation of connexin50 in mice results in microphthalmia and zonular pulverulent cataracts. J Cell Biol 1998;143(3):815–25. doi: 10.1083/jcb.143.3.815 [published Online First: 1998/11/13] [PubMed: 9813099]
55. Rong P, Wang X, Niesman I, et al. Disruption of Gja8 (alpha8 connexin) in mice leads to microphthalmia associated with retardation of lens growth and lens fiber maturation. Development 2002;129(1):167–74. doi: 10.1242/dev.129.1.167 [published Online First: 2002/01/10] [PubMed: 11782410]
56. Alizadeh A, Clark J, Seeberger T, et al. Characterization of a mutation in the lens-specific CP49 in the 129 strain of mouse. Invest Ophthalmol Vis Sci 2004;45(3):884–91. [PubMed: 14985306]
57. Simirskii VN, Lee RS, Wawrousek EF, et al. Inbred FVB/N mice are mutant at the cp49/Bfsp2 locus and lack beaded filament proteins in the lens. Invest Ophthalmol Vis Sci 2006;47(11):4931–4. doi: 10.1167/iovs.06-0423 [PubMed: 17065509]
58. Zhou Y, Bennett TM, Ruzycki PA, et al. Mutation of the EPHA2 Tyrosine-Kinase Domain Dysregulates Cell Pattern Formation and Cytoskeletal Gene Expression in the Lens. Cells 2021;10(10) doi: 10.3390/cells10102606 [published Online First: 2021/10/24] [PubMed: 35011571]
59. Zhou Y, Bennett TM, Shiels A. Mutation of the TRPM3 cation channel underlies progressive cataract development and lens calcification associated with pro-fibrotic and immune cell responses. FASEB J 2021;35(2):e21288. doi: 10.1096/fj.202002037R [published Online First: 2021/01/24] [PubMed: 33484482]

60. Shi Y, De Maria A, Bennett T, et al. A role for epha2 in cell migration and refractive organization of the ocular lens. Invest Ophthalmol Vis Sci 2012;53(2):551–9. doi: 10.1167/iovs.11-8568 [published Online First: 2011/12/15] [PubMed: 22167091]
61. Zhou Y, Shiels A. Epha2 and Efna5 participate in lens cell pattern-formation. Differentiation 2018;102:1–9. doi: 10.1016/j.diff.2018.05.002 [PubMed: 29800803]
62. Aaron JS, Taylor AB, Chew TL. Image co-localization - co-occurrence versus correlation. J Cell Sci 2018;131(3) doi: 10.1242/jcs.211847 [published Online First: 2018/02/14]
63. Schindelin J, Arganda-Carreras I, Frise E, et al. Fiji: an open-source platform for biological-image analysis. Nat Methods 2012;9(7):676–82. doi: 10.1038/nmeth.2019 [published Online First: 2012/06/30] [PubMed: 22743772]
64. Schroeder AB, Dobson ETA, Rueden CT, et al. The ImageJ ecosystem: Open-source software for image visualization, processing, and analysis. Protein Sci 2021;30(1):234–49. doi: 10.1002/pro.3993 [published Online First: 2020/11/10] [PubMed: 33166005]
65. Alam MS. Proximity Ligation Assay (PLA). Curr Protoc Immunol 2018;123(1):e58. doi: 10.1002/cpim.58 [published Online First: 2018/09/22] [PubMed: 30238640]
66. Lam PT, Padula SL, Hoang TV, et al. Considerations for the use of Cre recombinase for conditional gene deletion in the mouse lens. Hum Genomics 2019;13(1):10. doi: 10.1186/s40246-019-0192-8 [published Online First: 2019/02/17] [PubMed: 30770771]
67. White TW. Nonredundant gap junction functions. News Physiol Sci 2003;18:95–9. doi: 10.1152/nips.01430.2002 [published Online First: 2003/05/17] [PubMed: 12750443]
68. Cashikar AG, Shim S, Roth R, et al. Structure of cellular ESCRT-III spirals and their relationship to HIV budding. Elife 2014;3 doi: 10.7554/eLife.02184
69. Yamada K, Tomita HA, Kanazawa S, et al. Genetically distinct autosomal dominant posterior polar cataract in a four-generation Japanese family. Am J Ophthalmol 2000;129(2):159–65. [PubMed: 10682967]
70. Yamada K, Tomita H, Yoshiura K, et al. An autosomal dominant posterior polar cataract locus maps to human chromosome 20p12-q12. Eur J Hum Genet 2000;8(7):535–9. doi: 10.1038/sj.ejhg.5200485 [PubMed: 10909854]
71. Auth T, Schluter S, Urschel S, et al. The TSG101 protein binds to connexins and is involved in connexin degradation. Exp Cell Res 2009;315(6):1053–62. doi: 10.1016/j.yexcr.2008.12.025 [published Online First: 2009/02/13] [PubMed: 19210987]
72. Leithe E, Kjenseth A, Sirnes S, et al. Ubiquitylation of the gap junction protein connexin-43 signals its trafficking from early endosomes to lysosomes in a process mediated by Hrs and Tsg101. J Cell Sci 2009;122(Pt 21):3883–93. doi: 10.1242/jcs.053801 [published Online First: 2009/10/08] [PubMed: 19808888]
73. Totland MZ, Rasmussen NL, Knudsen LM, et al. Regulation of gap junction intercellular communication by connexin ubiquitination: physiological and pathophysiological implications. Cell Mol Life Sci 2020;77(4):573–91. doi: 10.1007/s00018-019-03285-0 [published Online First: 2019/09/11] [PubMed: 31501970]
74. Falk MM, Kells RM, Berthoud VM. Degradation of connexins and gap junctions. FEBS Lett 2014;588(8):1221–9. doi: 10.1016/j.febslet.2014.01.031 [published Online First: 2014/02/04] [PubMed: 24486527]
75. Gong X, Agopian K, Kumar NM, et al. Genetic factors influence cataract formation in alpha 3 connexin knockout mice. Dev Genet 1999;24(1-2):27–32. doi: 10.1002/(SICI)1520-6408(1999)24:1/2<27::AID-DVG4>3.0.CO;2-7 [published Online First: 1999/03/18] [PubMed: 10079508]
76. Gerido DA, Sellitto C, Li L, et al. Genetic background influences cataractogenesis, but not lens growth deficiency, in Cx50-knockout mice. Invest Ophthalmol Vis Sci 2003;44(6):2669–74. doi: 10.1167/iovs.02-1311 [published Online First: 2003/05/27] [PubMed: 12766071]
77. White TW. Unique and redundant connexin contributions to lens development. Science 2002;295(5553):319–20. doi: 10.1126/science.1067582 [published Online First: 2002/01/12] [PubMed: 11786642]

78. Sellitto C, Li L, White TW. Connexin50 is essential for normal postnatal lens cell proliferation. Invest Ophthalmol Vis Sci 2004;45(9):3196–202. doi: 10.1167/iovs.04-0194 [published Online First: 2004/08/25] [PubMed: 15326140]

79. Chai Z, Goodenough DA, Paul DL. Cx50 requires an intact PDZ-binding motif and ZO-1 for the formation of functional intercellular channels. Mol Biol Cell 2011;22(23):4503–12. doi: 10.1091/mbc.E11-05-0438 [published Online First: 2011/10/04] [PubMed: 21965293]

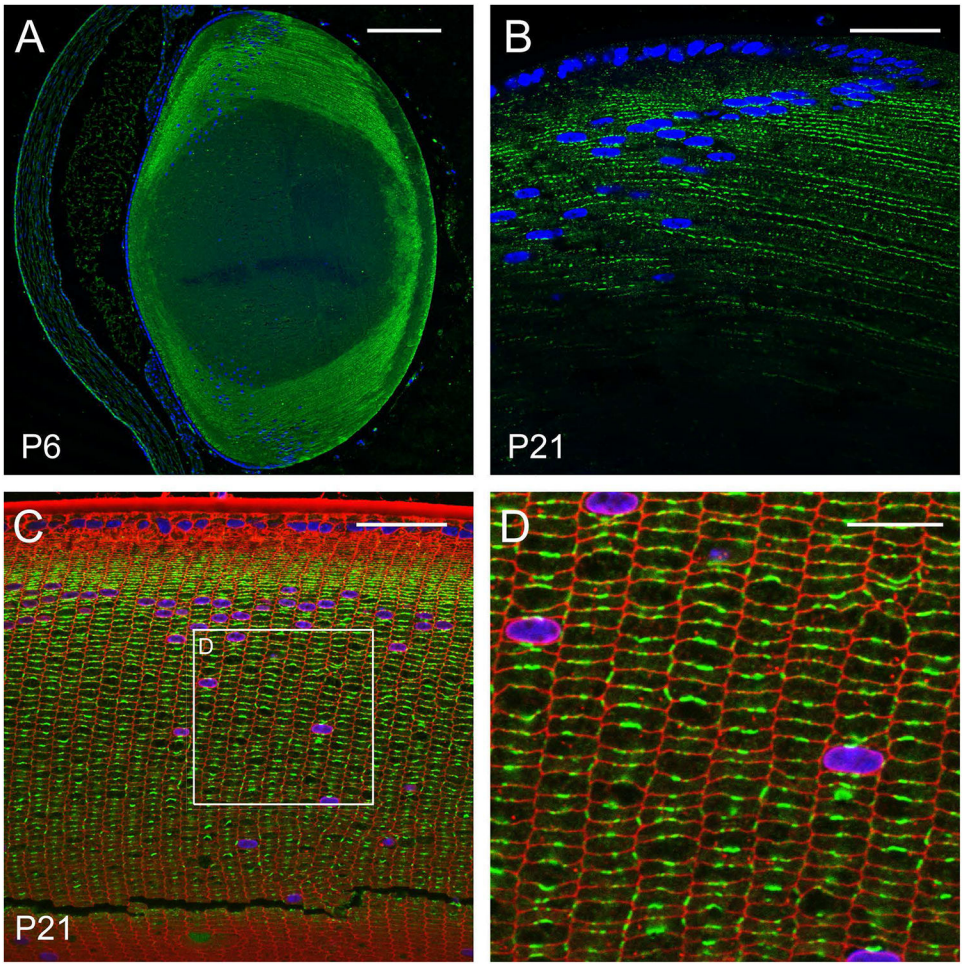

Figure 1. CHMP4B localization in the lens.

Representative IFCM images of the wild-type mouse lens at P6 (**A**) and P21(**B-D**) in the sagittal plane (**A, B**) and in cross-section (**C, D**) showing CHMP4B (green) localization to LFC membranes, particularly on the broad faces (D). Cell-membranes and nuclei were stained with WGA (red) and DAPI (blue), respectively. Scale bar: 100-μm (A), 30-μm (B, C), 15-μm (D).

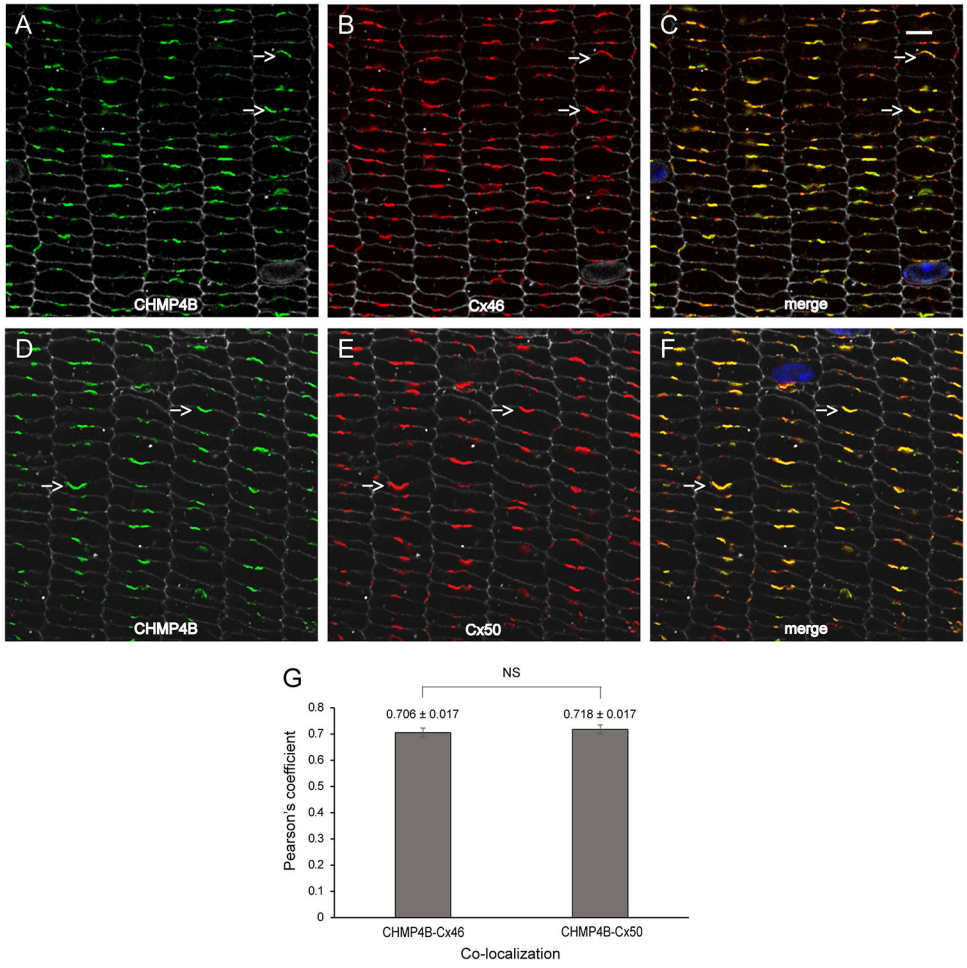

Figure 2. Co-localization of CHMP4B with gap-junction proteins Cx46 and Cx50 in the lens.

Representative IFCM images of CHMP4B (**A, C, D, F**), Cx46 (**B, C**), and Cx50 (**E, F**) distribution in cross-sections of the mouse lens (P28). White arrows indicate potential **B&S** structures rich in CHMP4B and Cx46 or Cx50 on the broad faces of LFC-membranes. Cell membranes were stained with WGA (white) and nuclei with DAPI (blue). Scale bar: 5-μm. (G) Quantification of CHMP4B co-localization with Cx46 and Cx50 in wild-type lenses calculated using Pearson's correlation coefficient. NS, not significant. Error bars represent SE.

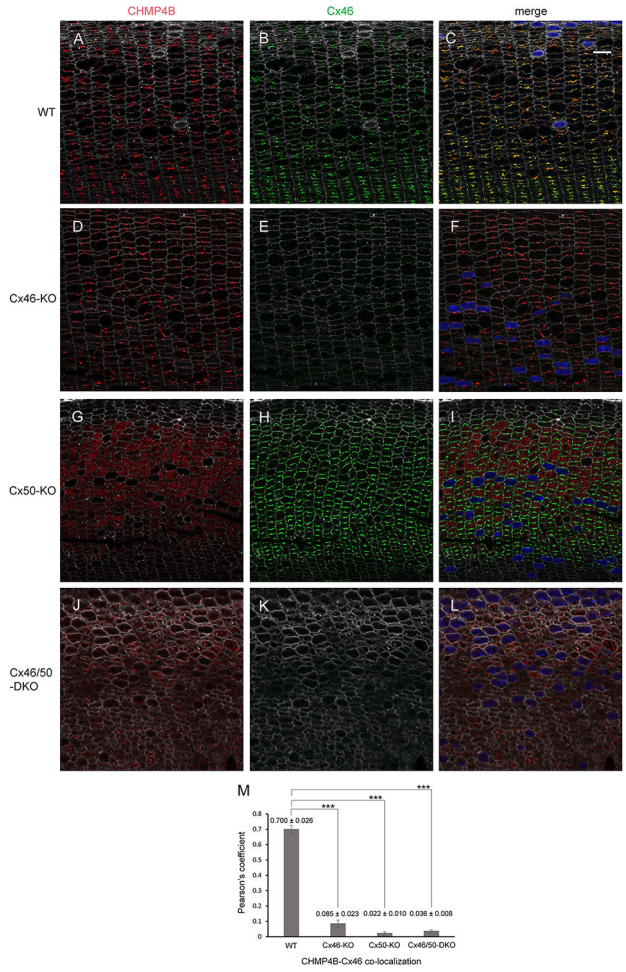

Figure 3. CHMP4B and Cx46 distribution in Cx46-KO, Cx50-KO, and Cx46/Cx50-DKO lenses.

Representative IFCM images of CHMP4B (**A, C, D, F, G, I, J, L**) and Cx46 (**B, C, E, F, H, I, K, L**) localization in lenses (P21) from wild-type (A-C), Cx46-KO (D-F), Cx50-KO (G-I), and Cx46/50-DKO (J-L) mice. Cell membranes were labelled with WGA (white) and nuclei with DAPI (blue). Scale bar: 10-μm. (**M**) Quantification of CHMP4B and Cx46 co-localization in wild-type, Cx46-KO, Cx50-KO, and Cx46/50-DKO lenses calculated using Pearson's correlation coefficient. ***$P \leq .001$. Error bars represent SE.

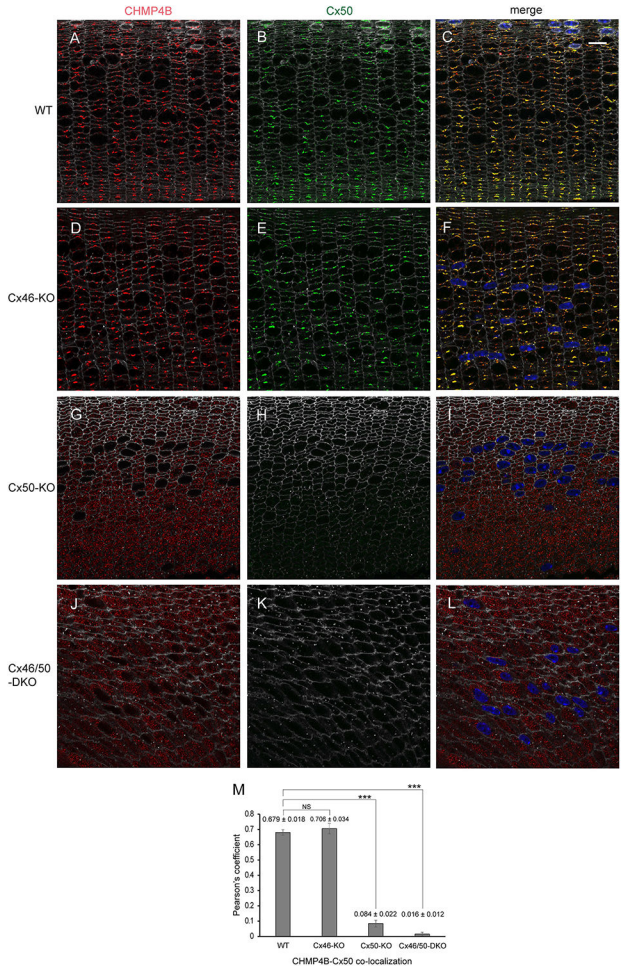

Figure 4. CHMP4B and Cx50 distribution in Cx46-KO, Cx50-KO, and Cx46/50-DKO lenses.

Representative IFCM images of CHMP4B (**A, C, D, F, G, I, J, L**) and Cx50 (**B, C, E, F, H, I, K, L**) localization in lenses (P21) from wild-type (A-C), Cx46-KO (D-F), Cx50-KO (G-I), and Cx46/50-DKO (J-L) mice. Cell membranes were labelled with WGA (white) and nuclei with DAPI (blue). Scale bar: 10-μm. (**M**) Quantification of CHMP4B and Cx50 co-localization in wild-type, Cx46-KO, Cx50-KO, and Cx46/50-DKO lenses calculated using Pearson's correlation coefficient. ***$P \leq .001$. NS, not significant. Error bars represent SE.

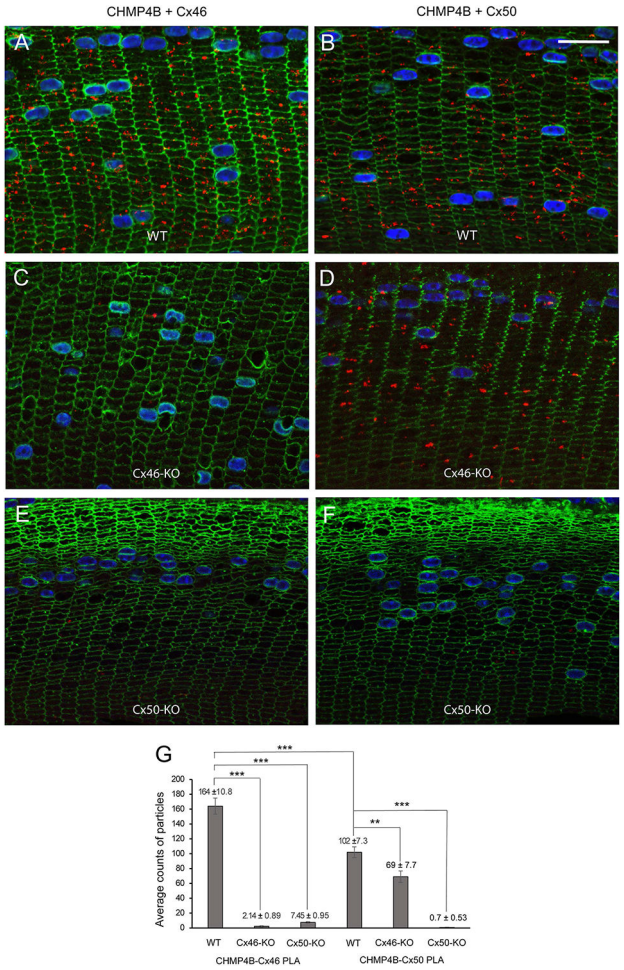

Figure 5. CHMP4B forms complexes with gap-junction proteins Cx46 and Cx50 in the lens.

(**A**-**D**) Representative IFCM images of mouse lens cross-sections (P28), following the *in situ* proximity ligation assay (PLA), showing complex-formation (red) between CHMP4B and Cx46 (**A**) and CHMP4B and Cx50 (**B**) in wild-type lenses. CHMP4B-Cx46 complexes were lost in Cx46-KO lenses (**C**), whereas, CHMP4B-Cx50 complexes were retained in Cx46-KO lenses (**D**). CHMP4B-Cx46 and CHMP4B-Cx50 complexes were both lost in Cx50-KO lenses (**E** and **F**). Scale bar: 20-μm. (**G**) Quantitation of PLA positive signals for CHMP4B-Cx46 and CHMP4B-Cx50 membrane complexes in wild-type versus Cx46-KO and Cx50-KO lenses. $^{**}P \leq .01$, $^{***}P \leq .001$. Error bars represent SE.

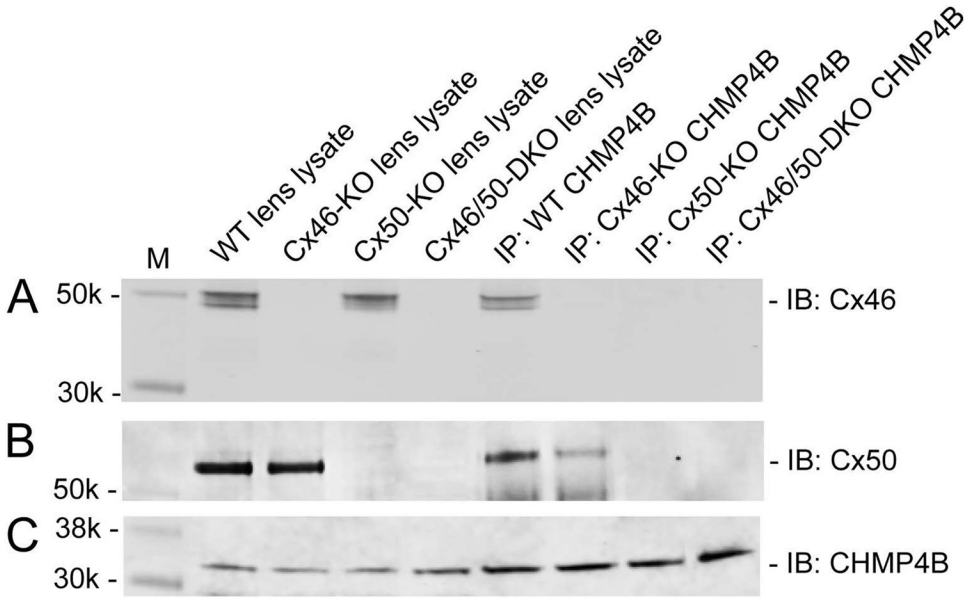

Figure 6. CHMP4B forms complexes with Cx46 and Cx50 *in vitro*.

(**A-C**) CHMP4B immuno-precipitation (IP) complexes from wild-type (WT), Cx46-KO, Cx50-KO, and Cx46/50-DKO mouse lens lysates immunoblotted (IB) with anti-Cx46 (A), anti-Cx50 (B), or anti-CHMP4B (C). Molecular size markers (mw).